Check for updates

Design and development of self-compacting alkali-activated concrete for energy-efficient building material

Bhagyashri A. Lanjewar [1]*, Abhilasha N. Kumbalwar[1],
Hindavi Gavali[2], Vaidehi A. Dakwale[1] and
Rahul V. Ralegaonkar [1]

[1]Department of Civil Engineering, Visvesvaraya National Institute of Engineering, Nagpur, India,
[2]NICMAR University, Pune, India

Anticipated urbanization and population growth, particularly in developing countries, are expected to boost demand for concrete, resulting in higher emissions and raw material consumption. In response to growing global sustainability awareness, various industries and countries have implemented diverse initiatives aimed at significantly reducing their greenhouse gas emissions. Alkali Activated Concrete (AAC), often known as zero cement concrete, is a viable substitute for conventional concrete. This study developed self-compacting alkali-activated concrete (SCAAC) using agro-industrial wastes and curing at ambient temperatures. The precursors were ground granulated blast furnace slag (GGBS) and fly ash (FA), which were activated with sodium hydroxide flakes and liquid sodium silicate. Co-fired bio-blended ash (BA), an agro-industrial waste, was used to partially replace river sand. The physical, chemical, mineral, and morphological properties of BA were thoroughly investigated. The BA was found suitable to use as a partial replacement for river sand in self-compacting alkali-activated concrete. The curing at ambient temperature was effective in producing a high-strength and durable concrete material. The thermal conductivity of the developed concrete was determined. The reduction in embodied energy for the developed material was calculated. The reduction in peak cooling load was found using computational modeling for cement based concrete and SCAAC. The developed concrete successfully met the specified compressive strength requirement for M30 grade concrete, achieving a value of 38.12 MPa. Reduction in embodied energy (7.37%) of the developed concrete was observed as compared to conventional concrete. Results show that the peak cooling load reduced by 35% compared to conventional concrete [1.9 W/(m.K)] due to the lower thermal conductivity of the developed material [1.247 W/(m.K)]. The use of agro-industrial wastes in the concrete mixture not only reduced the environmental impact but also utilized waste materials that would otherwise be disposed of in landfills. Overall, this study demonstrates the potential for sustainable and environmentally friendly construction materials using agro-industrial wastes.

KEYWORDS

alkali-activated concrete, self-compacting concrete, sustainable construction material, co-fired bio-blended ash, GGBS and FA

1 Introduction

According to United Nations projections (2018), approximately 68% of the global population is expected to reside in urban areas by 2050, reflecting an estimated 13% increase over the next 3 decades (United Nation, 2018; Chippagiri et al, 2022a). In light of current trends in rapid urbanization and population growth, a significant increase in concrete production and consumption is expected to meet the rising infrastructure demands. The International Energy Agency projects that global concrete demand will surpass 18 billion tons annually by 2050 (International Energy Agency Global Energy Review, 2022). This anticipated surge in concrete demand poses serious environmental challenges, as its production is closely linked to significant greenhouse gas (GHG) emissions and the excessive consumption of natural resources (Scrivener et al., 2018; Jittin and Bahurudeen, 2022). Cement, the primary binder in concrete, contributes over 7% of GHG emissions and stands as one of the leading industrial sources of CO_2 emissions (Supriya et al., 2023). A significant body of research is focused on developing alternatives to cement, which is the most energy-intensive component of concrete (Supriya et al., 2023; Lin et al., 2024; Wang et al., 2024; Dang et al., 2024; Hassan et al., 2024; Fernando et al., 2023; Law et al., 2023; Lian et al., 2023; Cheng et al., 2023; Adesina et al., 2022). Some of the alternatives being investigated include fly ash, slag, and silica fume, which have the potential to reduce the carbon footprint of concrete production (Abhishek et al., 2022; Lanjewar et al., 2023a; Chippagiri et al., 2021; Yoo et al., 2024; Ralegaonkar et al., 2017).

Alkali activated concrete is emerging as a sustainable alternative to cement and has shown promising results in terms of strength and durability, making it a viable construction material (Li et al., 2023; Ji et al., 2023; Cai et al., 2022; Yurt and Bekar, 2022; Yang et al., 2022; Tambara Júnior et al., 2022; Gavali et al., 2019; Gavali et al., 2021; Lanjewar et al., 2023b). Alkali activated material (AAM) is an amorphous three-dimensional aluminum-silicate binder material produced by reacting raw materials rich in SiO_2 and Al_2O_3 (precursors) with an alkaline solution (activator) (Jittin and Bahurudeen, 2022; Supriya et al., 2023). Alkali activation is a chemical process involving the dissolution of precursors in alkali activators (Lanjewar et al., 2023a). The alkaline activator polymerizes with the silica-aluminate binder material to produce a reticulated cementitious structure consisting of Si-O-Al-O bonds. Agro-industrial wastes, including fly ash (FA), silica fume (SF), metakaolin (MK), ground granulated blast furnace slag (GGBS), rice husk ash (RHA), sugarcane bagasse ash (SBA), and palm oil fuel ash (POFA), are the most widely used precursors (Kejkar et al., 2020; Nodehi and Taghvaee, 2022a; Nodehi and Taghvaee 2022b; shelote et al., 2021). The most commonly used alkali activators in the construction industry are sodium hydroxide and sodium silicate (Mohammed et al., 2021). This not only highlights the effectiveness of agro-industrial wastes as precursors but also underscores the potential of alkali-activated concrete as a sustainable alternative in the construction industry. Moreover, alkali-activated concrete has a lower carbon footprint than traditional cement, which enhances its environmental friendliness and aligns with sustainable construction practices (Unis Ahmed et al., 2022; Farhan et al., 2019; Robayo-Salazar et al., 2018). Its ability to reduce greenhouse gas emissions and decrease the reliance on finite natural resources has sparked interest around the world. Furthermore, widespread adoption of alkali activated concrete may necessitate significant changes in construction practices and regulations, posing challenges for large-scale implementation.

Combining the sustainability of alkali-activated concrete with the enhanced workability of self-compacting concrete offers a solution that reduces environmental impact while improving construction efficiency. Self-compacting concrete is distinguished by its ability to flow effortlessly into formwork, filling intricate spaces without requiring external vibration or compaction (Malazdrewicz et al., 2023). Self-compacting concrete is ideal for structures with dense reinforcement or complex shapes, as it ensures uniform distribution and reduces the risk of honeycombing or voids (Malazdrewicz et al., 2023). Self-compacting concrete is commonly utilized in off-site modular construction technology. Additionally, this type of concrete can improve construction efficiency and reduce labor costs, making it a popular choice for many construction projects.

The year 2050 holds immense significance for our planet, with industries worldwide actively pursuing innovative approaches to achieve net-zero emissions (Adesina, 2020). This effort is crucial in averting the rise of global temperatures to 1.5°C and beyond, as highlighted by the Intergovernmental Panel on Climate Change (IPCC) in 2018 (Wimbadi and Djalante, 2020; IPCC, 2018). The building industry is a major consumer of resources, including energy and materials. Buildings require energy both during construction (embodied energy associated with the acquisition and processing of building materials) and for operations to maintain a comfortable indoor atmosphere (Ballesty and Sawhney 2023). Extreme weather conditions have forced individuals to stay indoors in a confined atmosphere within a thermal comfort level (Chippagiri et al., 2022b; Ram et al., 2018). Temperature, controlled indoor air quality (IAQ), humidity, lighting, and noise levels are some of the factors that contribute to the growing concept of indoor environment quality (IEQ) (Chippagiri et al., 2022b). Space cooling, which accounts for 50%–70% of overall energy usage in commercial buildings, can be significantly reduced with efficient thermal insulation (Chippagiri et al., 2022c). Enhanced thermal insulation not only improves comfort but also saves energy that would otherwise be used for excessive heating or cooling, highlighting the critical significance of material selection in building energy conservation initiatives. The OPC in concrete design has high embodied energy and studies suggest that for each kilogram of manufactured cement, CO2 is released in the form of emissions between 0.66 and 0.82 kg. Self-compacting alkali-activated concrete (SCAAC) not only reduces carbon emissions by utilizing industrial by-products but also minimizes energy consumption during construction due to its self-consolidating nature, eliminating the need for mechanical vibration.

Self-compacting concrete made without cement can meet the requirements for rapid construction, waste utilization, and low carbon emissions. Despite the advancements in alkali-activated and self-compacting concrete technologies, limited research has explored their combined potential in developing energy-efficient building components. The integration of self-compacting alkali-activated concrete (SCAAC) into modular construction remains largely unexplored, particularly concerning its ability
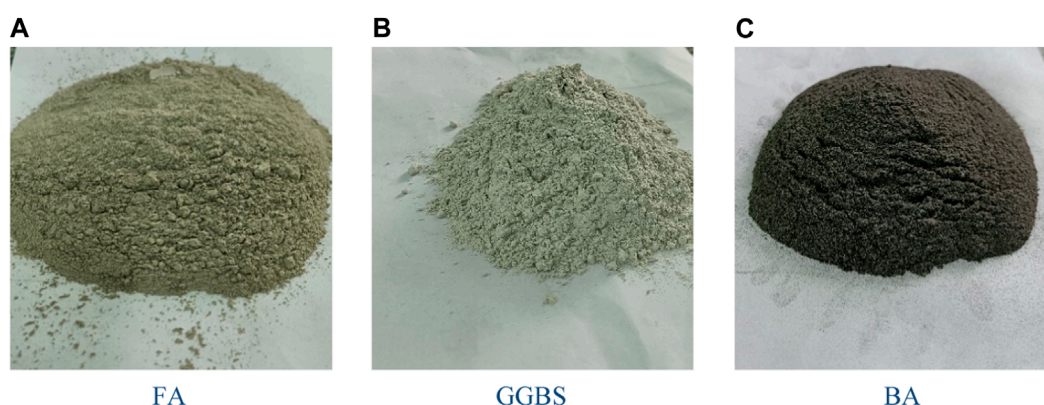
FIGURE 1
Raw Materials. **(A)** FA. **(B)** GGBS. **(C)** BA.

TABLE 1 Properties of materials used for concrete.

Physical properties	BA	Fly ash	GGBS
Colour	Black	Dark grey	Off-white
Specific gravity	2.29	2.54	2.85

to enhance thermal performance, reduce energy consumption, and extend the lifespan of structural elements. This study aims to address this research gap by investigating the viability of SCAAC modules as sustainable and energy-efficient solutions for modern building applications. It presents the design and development of alkali activated concrete utilizing the agro-industrial waste by products. The bio-based ash namely co-fired blended ash was used in the making of sustainable concrete. Fresh and hardened properties of concrete were observed. The energy analysis for SCAAC and conventional concrete is done to find out the reduction in embodied energy for the developed material.

2 Materials and methods

2.1 Raw materials

Alkali Activated Concrete consists of Precursor, binder, Fine aggregate and Coarse Aggregate as complied to IS 17452:2020 (Concrete for Precast, 2020). Fly ash and GGBS were used as precursor (Figures 1a, b). Commercially available sodium-based activators, i.e., sodium hydroxide flakes (NaOH) and liquid sodium silicate (Na_2SiO_3) were used as alkali activator binders. River sand was used as fine aggregate and was replaced with blended ash (BA) in appropriate proportions (Figure 1c). Blended ash is obtained from industry where coal and biomass-based fuel is co-fired to achieve heating temperature of 800°C as the operative boiler temperature. It was procured from paper mill near the study

region. Industry uses coal and rice-husk in the ratio of 1:9 for co-firing. Properties of raw material significantly affect the result of developed product.

Thus to ascertain the feasibility of raw materials, Physical properties (including particle size distribution, specific gravity), chemical composition (XRF), mineralogical phases (XRD), and morphological structure (SEM) were studied. Table 1 presents the physical properties of materials. Alkali activator precursors are typically alumino-silicate materials. As the XRF analysis results suggests in Table 2, GGBS has high content of SiO_2 and CaO (40% silicate, 42% calcium), which makes it suitable to be used as alkali activator precursor (Huseien and Shah, 2020). While FA was used as an alumina silicate source (4.7% calcium, 54.11% silicate, and 26.51% alumina) to compensate for the low alumina content in GGBS (4.1% alumina. BA is a siliceous material containing 94.52% silica (Table 2) and is used as replacement to fine aggregate. Table 3 shows the properties of alkali activators.

The XRD analysis of BA shows the amorphous nature of the ash, which improves the reaction of the mix (Figure 2). The silica was present as crystalline quartz, as indicated by the peaks around $2\Theta = 20°–30°$. The other weak humps show the amorphous nature of the BA. The morphology of blended ash is shown in Figure 3, and it was found to have fine pores and an asymmetrical structure, which made it lighter in weight (Lanjewar et al., 2023a).

2.2 Methods

To achieve optimum proportion of binders, precursor and aggregates, several combinations were designed, cast and tested.

First set of composition was designed for finding optimum ratio of precursor, binder and aggregates. Alkali activator binder solution was prepared 30 minutes before casting, with Sodium Silicate (Na_2SiO_3) and Sodium Hydroxide (NaOH) in a ratio of 1:1.5. Solution of NaOH (10M) was prepared 1 day prior to casting the specimens by dissolving NaOH flakes in water. GGBS and FA were used in a fixed ratio of 1:1. River sand was replaced with BA at the rates of 10%, 20%, 30%, and 40% by weight (Table 4). Aggregates were dry mixed and then binder was added to it slowly,

TABLE 2 Chemical composition of materials.

Material	Oxides	SiO_2	Al_2O_3	Fe_2O_3	K_2O	SO_3	CaO	TiO_2	MgO	P_2O_5	Na_2O	LOI
BA	(wt%)	94.51	-	0.464	2.739	0.718	1.317	0.101	0.96	0.32	0.32	-
Fly ash	(wt%)	54.11	26.51	6.4	0.87	1.29	4.7	-	1.04	-	2.22	2.85
GGBS	(wt%)	40	4.1	2	-	0.1	42	-	6.2	-	-	0.25

TABLE 3 Properties of alkali activators used in the concrete.

Alkali activators	Type	Colour	pH	Specific gravity
NaOH	Sodium Hydroxide- Flakes	White	13.5–14.5	2.1
Na_2SiO_3 (LSS)	Sodium Silicate in liquid form (32.8% silica +14.7% sodium oxide and 52.5% water)	Off-white	11.2	1.57

FIGURE 2
XRD graph of BA.

FIGURE 3
SEM image of BA.
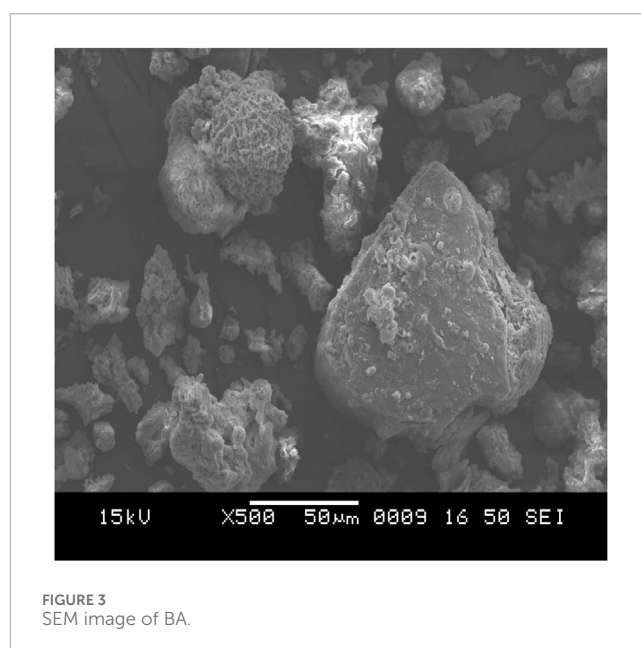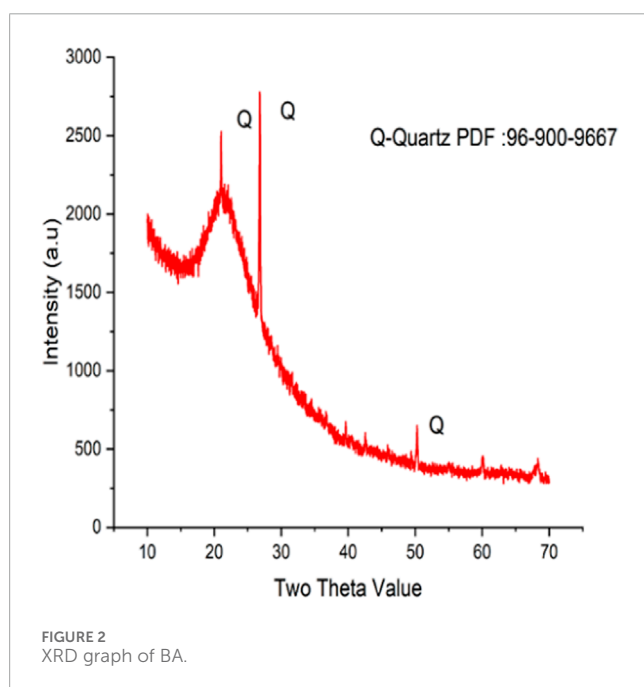
mixing time was approximately 3 minutes until homogeneous mix is achieved. 100 mm cube sample were cast. The samples were demolded after 24 h and cured at room-temperature until time of testing.

The second set of compositions was for designing self-compacting concrete (SCAAC) as per EFNARC (2002) guidelines (EFNARC, 2002). Four compositions were prepared with different molarities (8M, 10M, 12M, and 14M) for NaOH as given in Table 5. For attaining a non-segregating very high workability concrete, commercially available superplasticizer was used.

While casting, cracks have been observed on the surface of specimens in previous study (Lanjewar et al., 2023a); thus fibers (12 mm polypropylene fiber) were added to arrest the cracks.

The tests for SCAAC were done in accordance with the procedures specified in IS 1199 (Part 6) (Concrete Methods, 2018). T_{500}, slump-flow, V-funnel, L-box, and J-ring tests were performed sequentially. Self-compacting concrete must have the ability to fill voids by flowing into and through formwork on its self-weight. The slump flow measures the flow ability of the fresh concrete in an unconfined condition. Flow was noted when the concrete settled and spread diameter was constant. The t_{500} time is measured for observing relative viscosity of concrete. The T_{500} reading was taken when the flow reached a diameter of 500 mm.

In V-funnel test, duration of the concrete's flow through the V-funnel is noted. As per EFNARC, 2002 guidelines, it should be between 8 and 12 s. The concrete's ability to pass through narrow areas, such as between reinforcing bars, is determined using the L box test. The L-box's vertical section was filled with

TABLE 4 Compositions of mixes for 1 m³ of SCAAC (All values in kg).

Mix trial	NaOH molarity	FA	GGBS	BA	Fine aggregates	Coarse aggregates	AAS
S10C10	10M	300	300	46.7	420.3	933	415
S10C20	10M	300	300	93.4	373.6	933	415
S10C30	10M	300	300	140.1	326.9	933	415
S10C40	10M	300	300	186.8	280.2	933	415

TABLE 5 Mix proportion for SCAAC for 1 m³ of SCAAC (All values in kg).

Mix trial	NaOH molarity	FA	GGBS	BA	Fine aggregates	Coarse aggregates	Fiber (pp-12 mm)	Admixture (PCE based)	AAS
S8C10	8M	300	300	46.7	420.3	933	0.015 (0.25%)	0.030 (0.5%)	415
S10C10	10M	300	300	46.7	420.3	933	0.015 (0.25%)	0.030 (0.5%)	415
S12C10	12M	300	300	46.7	420.3	933	0.015 (0.25%)	0.030 (0.5%)	415
S14C10	14M	300	300	46.7	420.3	933	0.015 (0.25%)	0.030 (0.5%)	415

FIGURE 4
Slump flow.
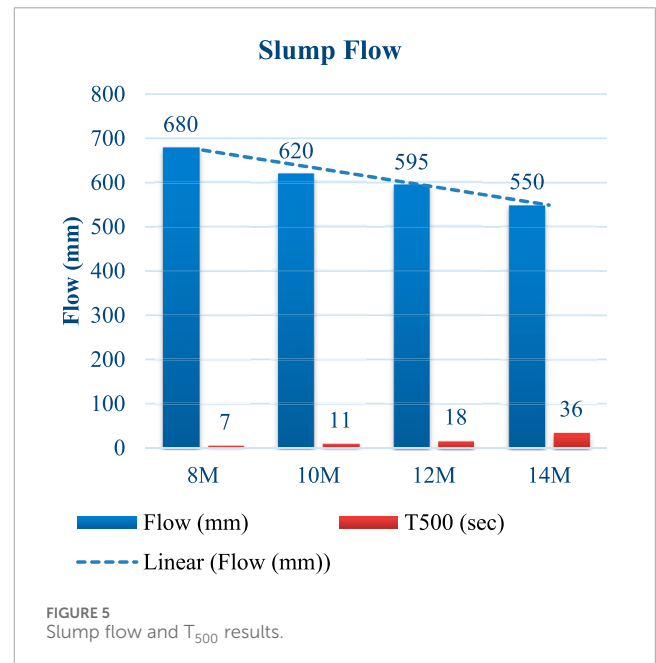
FIGURE 5
Slump flow and T_{500} results.

concrete and then leveled. The concrete was permitted to flow horizontally through the spaces between the vertical and smooth reinforcing bars when the sliding door was opened after 60 s. The height of concrete at vertical section (H1) and at the end of horizontal section (H2) was recorded and determined the H2/H1 ratio. The J ring test was also conducted to assess the passing ability of concrete.

For assessment of compressive strength the cube samples were cast in 100 mm cube moulds in compliance with

TABLE 6 Fresh properties of the concrete.

Sr No	Mix trial	NaOH molarity	Flow (mm)	T_{500} (sec)	V funnel (sec)	L box	J Ring (mm)
1	S8C10	8M	680	7	8.53	0.95	2
2	S10C10	10M	620	11	10.58	0.91	2
3	S12C10	12M	595	18	12.30	0.85	3
4	S14C10	14M	550	36	13.76	0.8	3
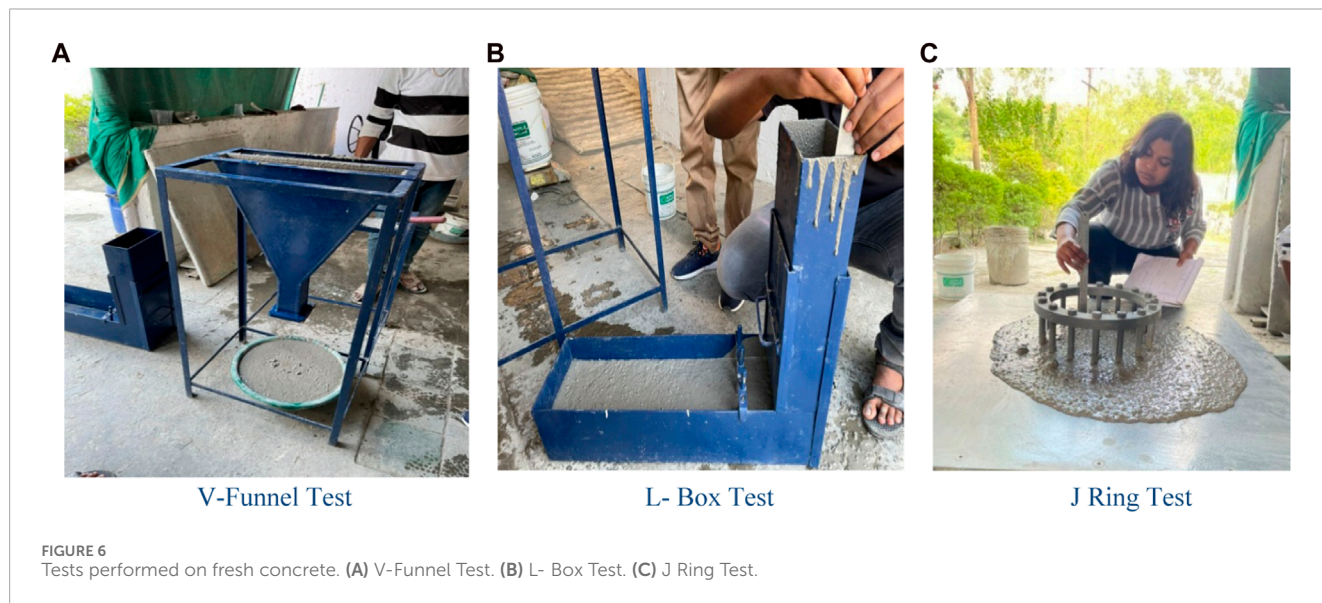
FIGURE 6
Tests performed on fresh concrete. **(A)** V-Funnel Test. **(B)** L- Box Test. **(C)** J Ring Test.
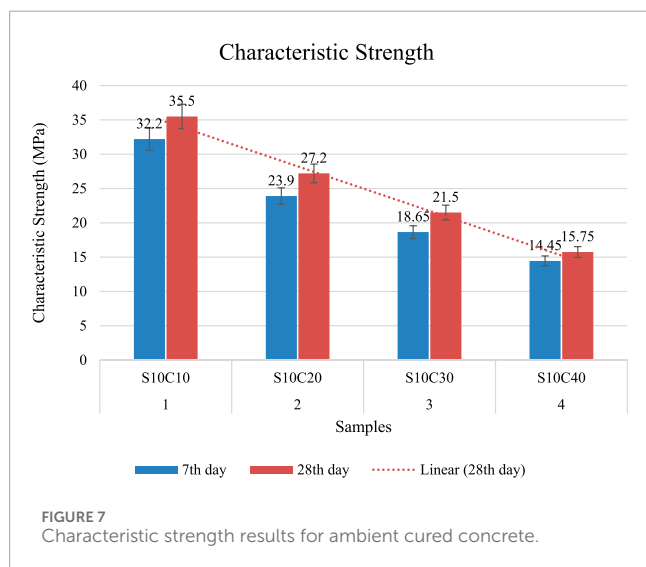
FIGURE 7
Characteristic strength results for ambient cured concrete.

IS 516:2018 (Concrete, 1959). For the split tensile test, 100 mm dia cylindrical specimens with h/d ration 1:2 and 100 × 100 × 500 mm beams were cast for flexural strength test. Further, three disc samples were cast for thermal conductivity test of the mix. All the test specimens were demolded after 24hrs and kept in room temperature for ambient curing.

3 Results and discussions

3.1 Fresh concrete properties

3.1.1 Slump flow

Slum flow it the primary desirable property of self-compacting concrete. It shows the flowability and resistance to segregation. According to EFNARC specifications, to achieve sufficient filling ability, the spread diameter of mix should be between 650 and 800 mm. Additionally, IS 10262:2019 (Indian Standard, 2019) has classified the slump flow in three categories SF1 (550–650 mm), SF2 (660–750 mm) and SF3 (760–850 mm). Result of slump flow test show that SCAAC mixes fall in the range of SF1 and SF2 (Figure 4) and thus suitable for lightly reinforced concrete structure to several structural applications such as slabs, beams and columns. It is evident that the molarity of NaOH influences the fresh properties of concrete significantly. As the molarity of NaOH increased, flow decreased. Flow value dropped from 680 to 550 when the NaOH molarity increased from 8 to 14 (Figure 5). As the concentration of SH increases, the viscosity of the NaOH solution increases. High concentration of NaOH accelerates the polymerization reaction, resulting in a early setting and lower workability for concrete. Slump flow test values for SCAAC with different molarities are given in Table 6.

FIGURE 8
Characteristic strength results for SCAAC.

FIGURE 9
Rapid chloride permeability test.
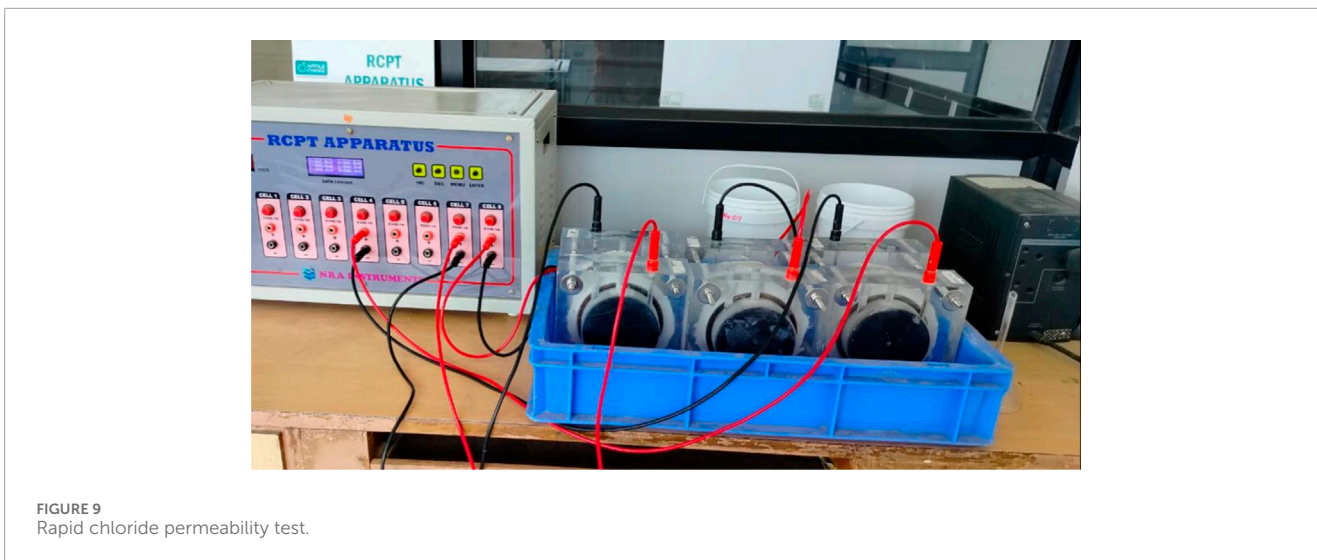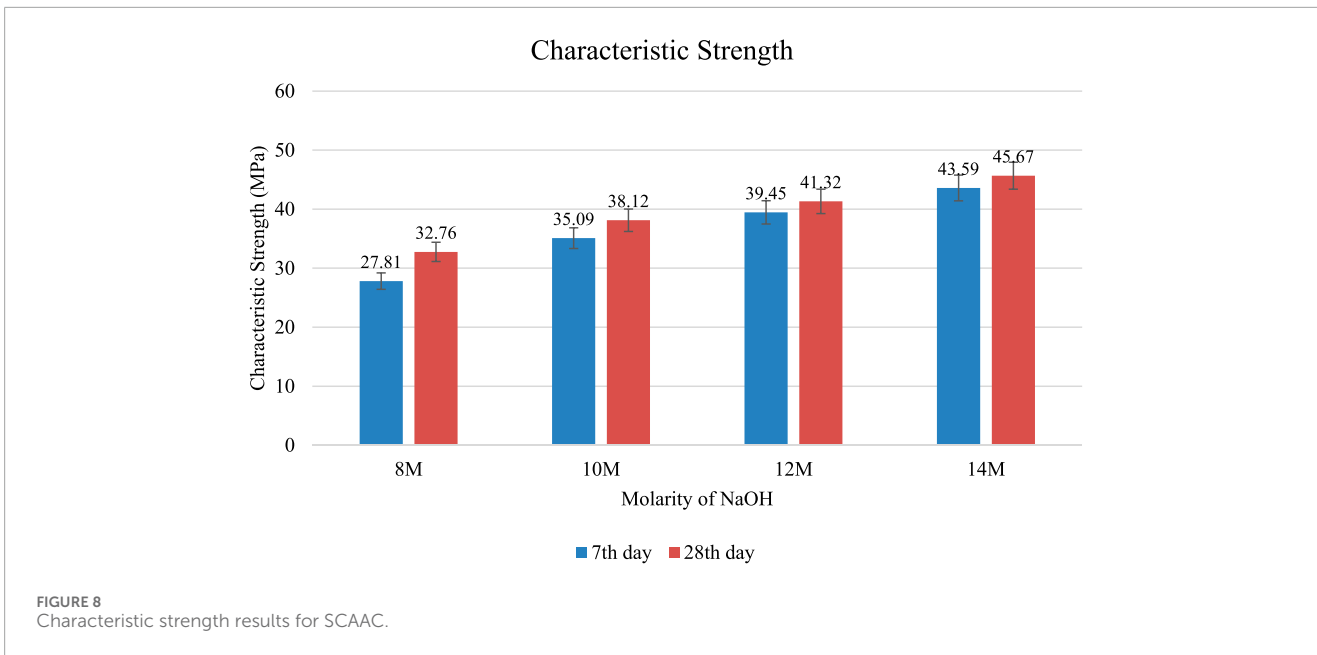
TABLE 7 Thermal Conductivity of a developed material.

Mix	M(kg)	S (j/kg°C)	dT/dt	x(m)	A (m²)	T_2 (°C)	T_1 (°C)	K(W/m.K)
S10C10	0.776	4186.1	0.0141	0.009	0.00785	99.4	57.3	1.247

3.1.2 V-funnel test

The viscosity of the concrete can be represented by the V-funnel flow duration (Figure 6a) and time taken to reach 500 mm spread diameter, i.e., T500 duration. As per EFNARC recommendation, V-funnel flow period should not be more than 12 s. Therefore, the findings in Table 6 show that specimens made with 12 M and 14 M do not meet the criteria. Based on the results obtained, all the mixes fall into the V2 classification specified in IS10262:2019 (Table 6). V1 viscosity classification can be used for heavy reinforced structures however, it has minimal resistance to segregation and bleeding. Meanwhile, V2 classification has minimal formwork pressure and high resistance to bleeding and segregation. The findings also show that V-funnel time appears to rise as molarity increases. A higher concentration of SH increases the viscosity of concrete, resulting in an extended V-funnel flow time.

3.1.3 L box and J ring test

The L-Box and J-Ring tests can be adopted to determine the passing ability of concrete (Figures 6b, c). According to the

TABLE 8 Comparison of embodied energy (Sathvik et al., 2023; Kejkar et al., 2020).

Material	SCAAC (kg/m³)	Cement based concrete (kg/m³)	EE (MJ/kg)	Total EE for	
				SCAAC (MJ/m³)	Cement based concrete (MJ/m³)
Cement	-	385	4.9	-	1886.5
Fly Ash	300	160	0.033	9.9	5.28
GGBS	300	-	0.857	257.1	-
Fine Aggregates	420.3	937.5	0.083	34.8849	77.8125
CFBA	46.7			0	
Coarse Aggregates	933	745.28	0.083	77.439	61.85824
Water	114.4	200	0	0	0
Sodium hydroxide Flakes	45	-	6.52	293.4	-
Liquid Sodium Silicate	230	-	5.37	1235.1	-
Admixture	3	5.8	12.6	37.8	73.08
Total				1945.62	2104.53
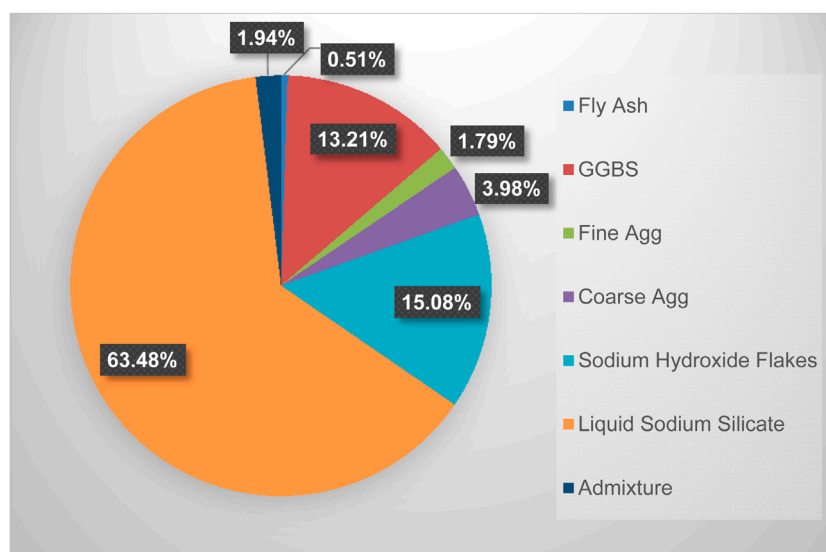
FIGURE 10
Percentage contribution of the raw materials in total EE for SCAAC.

EFNARC standard, the H2/H1 ratio should be between 0.8 and 1. Similarly, for the J Ring test, the height of concrete is measured within and outside the ring. The greater the difference in height, lesser the passing ability of concrete. J Ring test was performed in the combination with slump flow. According to the results, the H2/H1 ratio for all of the mixes ranges between 0.8 and 1. Similarly, for J Ring test, the difference in height ranges between 2 and 3 mm.

3.2 Mechanical concrete properties

3.2.1 Characteristic strength

After cubes were kept out in the open for ambient curing, characteristic strength testing was done on the 7th and 28th days to determine the hardness of concrete in accordance with IS 516: 1959 (Figure 7) (Concrete, 1959). The influence of bio-based ash on the strength of AAC was observed. The sand was substituted by 10, 20,
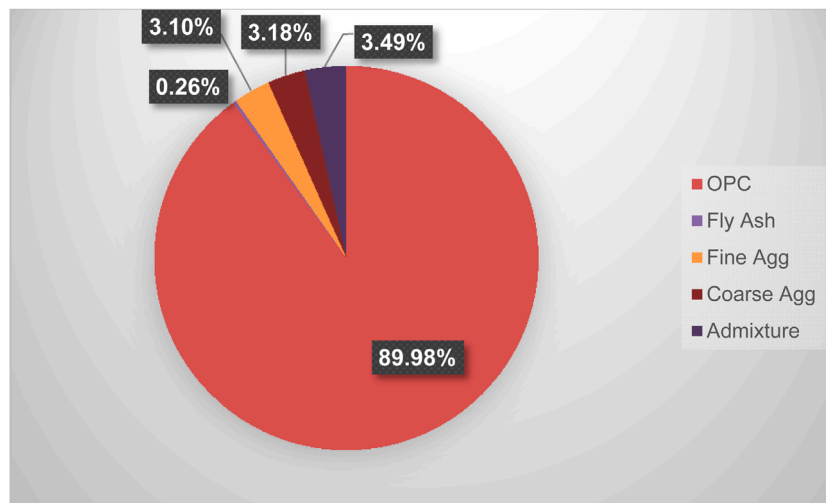
FIGURE 11
Percentage contribution of the raw materials in total EE for conventional concrete.

TABLE 9 Material properties of concrete for BIM analysis.

Case	Density (kg/m^3)	Compressive strength- 28th day (MPa)	Thermal conductivity (W/(m.K))
Conventional Concrete	2500	38	1.9
Developed Concrete	2350	38.12	1.247
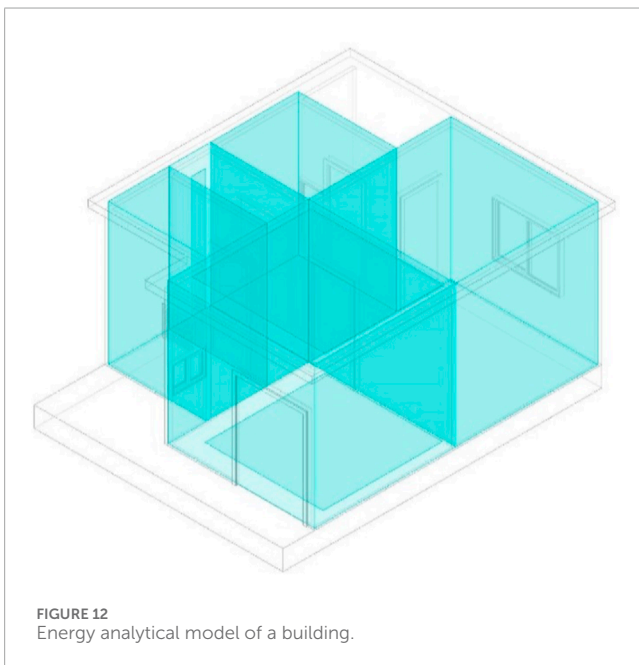
FIGURE 12
Energy analytical model of a building.

FIGURE 13
Comparison of peak cooling loads.

30, and 40 percentages by weight. With an increase in substitution %, the concrete's strength decreased. By increasing the BA percent from 10% to 20%, the strength reduced by 23.38%. Strength further dropped by 20.95% when percentage increased from 20% to 30%.

Furthermore, strength dropped by 26.74% when the percentage was raised from 30% to 40%. The maximum characteristic strength was found with 10% replacement, as shown in Figure 12, and this was chosen as the ideal proportion of BA to be used in concrete.

For self-compacting alkali activated concrete (SCAAC), according to observations, characteristic strength of 30–45 MPa was

TABLE 10 Cost Comparison of SCAAC and Cement based concrete.

Material	Unit cost (INR)	SCAAC		Cement based concrete	
		Quantity (kg/m^3)	Cost	Quantity (kg/m^3)	Cost
Cement	9.5	0	0	385	3657.5
Fly Ash	0.5	300	150	165	82.5
GGBS	1	300	300	0	0
Fine Aggregates	0.7	420.3	294.21	782	547.4
CFBA	0.5	46.7	23.35	0	0
Coarse Aggregates	0.9	933	839.7	804	723.6
Water	0.12	114.4	13.728	200	24
Sodium hydroxide Flakes	22	45	990	0	0
Liquid Sodium Silicate	12	230	2760	0	0
Admixture	70	3	210	5.8	406
Water for curing	0.12	0	0	600	72
Total			5580.988		5513

attained with a binder content of 600 kg/m^3, as shown in Figure 8. As generally observed in an alkali-activated concrete system, early-age strength have been obtained in case of all the mixes. Almost 90% of strength was achieved on the seventh day itself. Figure 13 shows the increase in the characteristic strength with an increase in the molarity of NaOH in the trials.

The specimens made with 10M solution resulted in the characteristic strength of 38.12 MPa, 14.06% more than the specimens made with 8M solution. Similarly, the strength of the specimens made with 14M solution was 45.67 MPa, 9.52% greater than the specimens made with 12M solution. A rise in the molarity of NaOH causes an increase in the concentration of OH$^-$, which helps the dissolution of silicates and aluminates from the precursors (Athira et al., 2021). A high concentration of hydroxyl ions causes the breaking of Ca-O, Al-O, and Si-O bonds in the GGBS, releasing Ca^{2+} ions and Si(OH)$_3$O$^-$, Si(OH)$_4$, and Al(OH)$^-_4$ monomers, which speeds up the formation of reaction products. This enhances polymerization, which results in higher strength (Li et al., 2023). The trial mix made with 10M solution was selected as the optimum mix as it achieved the target strength with the required fresh properties of concrete.

3.2.2 Split tensile and flexural strength

In accordance with IS 5816:1999, the optimal mix proportion was used while casting the cylindrical test specimens for the split tensile strength test. The samples were kept in lab (ambient temperature) for 28 days. Auto pacer compression testing machine with a capacity of 3000 KN was used for testing. The test specimens were placed in the center with steel rods carefully positioned along the top and bottom of the loading plane. The average split tensile strength obtained on the 28th

day was 3.95 MPa and found to be greater than 1/10th of characteristic strength.

Similarly, $100 \times 100 \times 500$ mm beams were cast for the flexural strength test with an optimum mix. Beams were subjected to a 2 point bending load. The average flexural strength obtained was 4.12 MPa, satisfying the IS 456:2000 flexural strength requirements.

3.2.3 RCPT

Samples with 50 mm thickness and 100 mm diameter were cast with the optimum mix proportion. After 28 days, samples were subjected to the Rapid Chloride Permeability Test (RCPT) in compliance with ASTM C1202 (Figure 9). Prior to testing, samples were covered with epoxy and vacuum saturated for 24 h (Fernando et al., 2023; Law et al., 2023). Sodium chloride (3% by mass in distilled water) and sodium hydroxide (0.3 N in distilled water) solutions were used as a reagents. Based on the prior studies, the voltage of 10V was applied (Fernando et al., 2023; Law et al., 2023). After 6 hours, the charge passed in was recorded in coulombs. A total charge of 928.7 ± 316.8°C was passed through the specimens. The results of the test showed that the concrete had a low chloride permeability, indicating good durability and resistance to corrosion.

3.2.4 Thermal conductivity

Extreme weather conditions have forced individuals to stay indoors in a confined atmosphere within a thermal comfort level (Chippagiri et al., 2022b). Temperature, controlled indoor air quality (IAQ), humidity, lighting, and noise levels are some of the factors that contribute to the growing concept of indoor environment quality (IEQ) (Chippagiri et al., 2022b). Thermal

conductivity is the ability of a material to conduct heat. Lower the thermal conductivity of the material, higher the thermal resistance (Gava and Ralegaonkar, 2018). The thermal performance of alkali activated concrete was computed for the optimum mix design. The laboratory experiment of thermal conductivity (k) was conducted with Lee's disc apparatus (Table 7). The thermal conductivity of developed concrete was noted to be lower when compared to that of conventional concrete. The k value of the developed material was obtained as 1.247 W/(m.K) which is 34.36% lower than conventional concrete [1.9 W/(m.K)]. The primary factors that affect thermal conductivity are the material's density, porosity, and moisture content.

The resulted values were found in accordance with IS 10262:2019 (Indian Standard, 2019) and EFNARC (EFNARC, 2002) standard. The advantage of proposed material i.e., alkali activated self-compacted concrete (AASCC) is that the target strength (30 MPa) is achieved in 7 days with zero water requirement for curing. The cited literature indicated the study related to recycled aggregate (Malazdrewicz et al., 2023) and use of GGBS and FA (Huseien and Shah, 2020) application for SCC with use of cement as binder. Also, earlier cited works indicated the strength at the age of 28 days. Thus, the presented approach of developing the product has final strength at early age.

4 Energy analysis and costing

The promotion of low-energy, sustainable construction techniques and low-cost is crucial for achieving the government's housing targets (Tiwari, 2001), as highlighted during an industry focus group meeting with the Indian Concrete Institute (ICI) and industrial partners (Bras et al., 2020). Energy analysis is performed for evaluating the embodied energy and operating energy. The embodied energy is oftenly associated with the energy that is being used during the raw material extraction, production of end product and transportation. However, the operating energy is associated with the energy that is required to meet the cooling/heating demand during the occupancy. In order to control the conventional energy demand for the operation and in turn controlling the carbon footprint the designers need to evaluate the performance of built forms.

4.1 Embodied energy and cost analysis

Energy conservation is currently a priority in the making of eco-friendly construction materials. To evaluate the energy efficiency of the developed end product, embodied energy (EE) was calculated. The embodied energy was calculated for SCAAC and conventional concrete to produce 1 cubic meter of concrete. The mix composition for cement based concrete was developed for M30-grade self-compacting concrete in accordance with IS 10262: 2019 (Indian Standard, 2019). The EE required to produce 1 kg of material was determined (Table 8). The raw material emission variables were considered from the prior studies executed by Sathvik et al. (2023) and Kejkar et al. (2020). The total EE for SCAAC was observed to be 1945.62 MJ/m^3, while for conventional concrete it was 2104.53 MJ/m^3. As per the results, the embodied

energy is reduced by 7.55% for developed concrete as compared to conventional concrete. Alkali activators significantly contribute to the embodied energy of SCAAC. Sodium silicate is a major contributor, accounting for around 63% of the total EE (Figure 10). Meanwhile, cement accounts for almost 90% of total EE in conventional concrete (Figure 11).

4.2 Peak cooling load analysis

In India, there is a significant variation in household electrical consumption patterns among states. In March 2019, the Indian government introduced the India Cooling Action Plan (ICAP), a 20-year initiative aimed at addressing building cooling requirements. Energy-saving measures in the building have mostly focused on improving the energy efficiency of the building's heating and cooling technologies. In order to increase thermal comfort and lower the need for mechanical cooling in buildings, innovative design of buildings using sustainable, clean materials may significantly reduce the impact on the environment, energy, and economics.

The effect of material selection on peak cooling load was studied by considering a case involving a housing development plan that comes under a slum rehabilitation scheme located in Nagpur, India (21.1232° N, 79.0515° E). This area falls under the composite climate zone geographically. The computational building model was prepared using the BIM tool- Revit. It consists of three room-bedroom, living and kitchen with water closet. The developed model was considered for conventional concrete and alkali-activated concrete, and the material properties (Table 9) of the same were fed into the database. On the basis of heat gain through building elements, the peak cooling load was calculated by analysing the Revit model (Figure 12). The energy needed for the living room was more than that of the bedroom and kitchen since the peak cooling load value varies with space volume (Figure 13). The overall reduction is about 35% for developed concrete as compared to the base case due to the lower thermal conductivity of the material [1.247 W/(mK)].

4.3 Cost estimation

Along with the environmental benefits, the developed concrete is assessed for the cost estimate and compared with cement-based concrete (Table 10). Transportation, local availability, and market demand all contribute to the cost of concrete. Agro-industrial by-products are to be transported from the source to the concrete mix plant. The material costs shown in Table 9 are as per local market rates. The total water required for curing the cement-based concrete for 7 days will be 600 L. For 1 m^3 of concrete, the estimated cost is found to be competitive with that of cement-based concrete. Based on the estimate, SCAAC is found to be a potential alternative as an eco-friendly and cost competitive construction material.

5 Conclusion

This study has investigated the effect co-fired bio-based blended ash (BA) on the properties of SCAAC. Specifically, the fresh and mechanical properties.

- The incorporation of 10%–40% BA has reduced the characteristic strength from 35.5 MPa to 15.75 MPa. Adding GGBS has improved the early-age strength of concrete. Adding 10% of BA as a replacement for river sand was found to be most effective in the production of M30 grade ambient cured alkali-activated concrete.
- The PCE-based admixture performed effectively with the alkali activator solution to improve flow.
- The molarity of NaOH has a major influence on the fresh concrete properties. The flow decreased from 680mm to 550 mm as the molarity increased from 8 to 14 M. As the molarity of the concrete increases, it becomes more cohesive.
- Similarly, the characteristic strength of concrete varied as the molarity of NaOH increased. The results revealed that the higher the molarity, the greater the characteristic strength.
- The thermal performance of the proposed material is found to be better than conventional concrete, with lower thermal conductivity.
- Reduction in embodied energy (7.55%) of the developed concrete was observed as compared to conventional concrete.
- The peak cooling load can be reduced by 35% compared to conventional concrete [1.9 W/(m.K)] due to the lower thermal conductivity of the developed material [1.247 W/(m.K)].

Data availability statement

The raw data supporting the conclusions of this article will be made available by the authors, without undue reservation.

Ethics statement

Written informed consent was obtained from the individual(s) for the publication of any potentially identifiable images or data included in this article.

Author contributions

BL: Conceptualization, Data curation, Formal Analysis, Investigation, Methodology, Resources, Visualization, Writing–original draft, Writing–review and editing. AK: Writing–review and editing. HG: Data curation, Formal Analysis, Software, Writing–review and editing. VD: Supervision, Visualization, Writing–review and editing. RR: Conceptualization, Funding acquisition, Investigation, Resources, Supervision, Validation, Visualization, Writing–review and editing.

Conflict of interest

The authors declare that the research was conducted in the absence of any commercial or financial relationships that could be construed as a potential conflict of interest.

The author(s) declared that they were an editorial board member of Frontiers, at the time of submission. This had no impact on the peer review process and the final decision.

Publisher's note

All claims expressed in this article are solely those of the authors and do not necessarily represent those of their affiliated organizations, or those of the publisher, the editors and the reviewers. Any product that may be evaluated in this article, or claim that may be made by its manufacturer, is not guaranteed or endorsed by the publisher.

References

Abhishek, H. S., Prashant, S., Kamath, M. V., and Kumar, M. (2022). Fresh mechanical and durability properties of alkali-activated fly ash-slag concrete: a review. *Innov. Infrastruct. Solut.* 7, 116. doi:10.1007/s41062-021-00711-w

Adesina, A. (2020). Recent advances in the concrete industry to reduce its carbon dioxide emissions. *Environ. Challenges* 1, 100004. doi:10.1016/j.envc.2020.100004

Adesina, A., de Azevedo, A. R. G., Amin, M., Hadzima-Nyarko, M., Agwa, I. S., Zeyad, A. M., et al. (2022). Fresh and mechanical properties overview of alkali-activated materials made with glass powder as precursor. *Clean. Mater.* 3, 100036. doi:10.1016/j.clema.2021.100036

Athira, V. S., Charitha, V., Athira, G., and Bahurudeen, A. (2021). Agro-waste ash based alkali-activated binder: cleaner production of zero cement concrete for construction. *J. Clean. Prod.* 286, 125429. doi:10.1016/j.jclepro.2020.125429

Bras, A., Ravijanya, C., de Sande, V. T., Rley, M., and Ralegaonkar, R. V. (2020). Sustainable and affordable prefab housing systems with minimal whole life energy use. *Energy Build.* 220, 110030. doi:10.1016/j.enbuild.2020.110030

Cai, R., Tian, Z., and Ye, H. (2022). Durability characteristics and quantification of ultra-high strength alkali-activated concrete. *Cem. Concr. Compos.* 134, 104743. doi:10.1016/j.cemconcomp.2022.104743

Ballesty, S., and Sawhney, A. (2023). Decarbonisation of the Built Environment: Using integrated life cycle and carbon emissions reporting. IOP Conference Series: Earth and Environmental Science, 1176 (1), 012046. doi:10.1088/1755-1315/1176/1/012046

Cheng, H., Chen, P., Rong, X., Cao, S., and Zhao, W. (2023). Effect of steel fibre and manufactured sand on mechanical properties of alkali-activated slag green cementitious material after high temperature. *Case Stud. Constr. Mater.* 18, e01919. doi:10.1016/j.cscm.2023.e01919

Chippagiri, R., Bras, A., Sharma, D., and Ralegaonkar, R. V. (2022a). Technological and sustainable perception on the advancements of prefabrication in construction industry. *Energies* 15, 7548. doi:10.3390/en15207548

Chippagiri, R., Bras, A., Sharma, D., and Ralegaonkar, R. V. (2022b). Technological and sustainable perception on the advancements of prefabrication in construction industry. *Energies* 15, 7548. doi:10.3390/en15207548

Chippagiri, R., Gavali, H. R., Bras, A., and Ralegaonkar, R. V. (2022c). Performance evaluation of a sustainable prefabricated system using small-scale experimental model technique. *Buildings* 12, 2000. doi:10.3390/buildings12112000

Chippagiri, R., Gavali, H. R., Ralegaonkar, R. V., Riley, M., Shaw, A., and Bras, A. (2021). Application of sustainable prefabricated wall technology for energy efficient social housing. *Sustain* 13 (3), 1195. doi:10.3390/su13031195

Concrete (1959). *IS 516 method of tests for strength of concrete*. Bur. Indian Stand., 1–30.

Concrete for Precast (2020). *Use of alkali activated concrete for Precast products - guidelines*. New Delhi: Bur. Indian Stand.

Concrete Methods (2018). *Bureau of Indian standard fresh concrete methods of sampling, testing and analysis*, 1199.

Dang, J., Tang, X., Xiao, J., and Han, A. (2024). Influence of alkaline activator and precursor on the foam characterization and alkali-activated foamed concrete properties. *Cem. Concr. Compos.* 145, 105341. doi:10.1016/j.cemconcomp.2023.105341

EFNARC (2002). *Design of self-compacting Concrete with fly ash*.

Farhan, N. A., Sheikh, M. N., and Hadi, M. N. S. (2019). Investigation of engineering properties of normal and high strength fly ash based geopolymer and alkali-activated slag concrete compared to ordinary portland cement concrete. *Constr. Build. Mater.* 196, 26–42. doi:10.1016/j.conbuildmat.2018.11.083

Fernando, S., Gunasekara, C., Law, D. W., Nasvi, M. C. M., Setunge, S., and Dissanayake, R. (2023). Assessment of long term durability properties of blended fly ash-rice husk ash alkali activated concrete. *Constr. Build. Mater.* 369, 130449. doi:10.1016/j.conbuildmat.2023.130449

Gava, H. R., and Ralegaonkar, R. V. (2018). Application of information modelling for sustainable urban-poor housing in India. *Proc. Inst. Civ. Eng. Sustain.* 172, 68–75. doi:10.1680/jensu.18.00015

Gavali, H. R., Bras, A., Faria, P., and Ralegaonkar, R. V. (2019). Development of sustainable alkali-activated bricks using industrial wastes. *Constr. Build. Mater.* 215, 180–191. doi:10.1016/j.conbuildmat.2019.04.152

Gavali, H. R., Bras, A., and Ralegaonkar, R. V. (2021). Cleaner construction of social housing infrastructure with load-bearing alkali-activated masonry. *Clean. Technol. Environ. Policy* 23, 2303–2318. doi:10.1007/s10098-021-02138-4

Hassan, A., ElNemr, A., Goebel, L., and Koenke, C. (2024). Effect of hybrid polypropylene fibers on mechanical and shrinkage behavior of alkali-activated slag concrete. *Constr. Build. Mater.* 411, 134485. doi:10.1016/j.conbuildmat.2023.134485

Huseien, G. F., and Shah, K. W. (2020). Durability and life cycle evaluation of self-compacting concrete containing fly ash as GBFS replacement with alkali activation. *Constr. Build. Mater.* 235, 117458. doi:10.1016/j.conbuildmat.2019.117458

Indian Standard (2019). *Indian standard, concrete mix proportioning – guidelines (second revision) IS 10262 2019*, New Delhi, India: Bureau of Indian Standards. 1–42.

International Energy Agency Global Energy Review (2022). *CO2 emissions in 2021 global emissions rebound sharply to highest ever level*. Paris, France: Iea, 1–14.

IPCC. (2018). *IPCC global warming of 1.5°C: an IPCC special Report on impacts of global warming of 1.5°C above pre-industrial levels in context of strengthening response to climate change, sustainable development, and efforts to eradicate pover*. Glob. Warm. 1.5°C 1–24.

Ji, X., Gu, X., Wang, Z., Xu, S., and Jiang, H. (2023). Admixture effects on the rheological/mechanical behavior and micro-structure evolution of alkali-activated slag backfills. *Minerals*. 13(1), 30. doi:10.3390/min13010030

Jittin, V., and Bahurudeen, A. (2022). Evaluation of rheological and durability characteristics of sugarcane bagasse ash and rice husk ash based binary and ternary cementitious system. *Constr. Build. Mater.* 317, 125965. doi:10.1016/j.conbuildmat.2021.125965

Kejkar, R. B., Madhukar, A., Agrawal, R., and Wanjari, S. P. (2020). Performance evaluation of cost-effective non-autoclaved aerated geopolymer (NAAG) blocks. *Arab. J. Sci. Eng.* 45, 8027–8039. doi:10.1007/s13369-020-04581-9

Lanjewar, B. A., Chippagiri, R., Dakwale, V. A., and Ralegaonkar, R. V. (2023a). Development of bio-based blended ash and fly ash based alkali activated concrete. *Mag. Concr. Res.* 75, 1202–1211. doi:10.1680/jmacr.22.00251

Lanjewar, B. A., Chippagiri, R., Dakwale, V. A., and Ralegaonkar, R. V. (2023b). Application of alkali-activated sustainable materials: a step towards net zero binder. *Energies* 16, 969. doi:10.3390/en16020969

Law, D., Patrisia, Y., Gunasekara, C., Castel, A., Nguyen, Q. D., and Wardhono, A. (2023). Durability assessment of alkali-activated concrete exposed to a marine environment. *J. Mater. Civ. Eng.* 35, 1–11. doi:10.1061/jmcee7.mteng-14346

Li, L., Xie, J., Zhang, B., Feng, Y., and Yang, J. (2023). A state-of-the-art review on the setting behaviours of ground granulated blast furnace slag- and

metakaolin-based alkali-activated materials. *Constr. Build. Mater.* 368, 130389. doi:10.1016/j.conbuildmat.2023.130389

Lian, C., Wang, Y., Liu, S., Hao, H., and Hao, Y. (2023). Experimental study on dynamic mechanical properties of fly ash and slag based alkali-activated concrete. *Constr. Build. Mater.* 364, 129912. doi:10.1016/j.conbuildmat.2022.129912

Lin, J. X., Liu, R. A., Liu, L. Y., Zhuo, K. Y., Chen, Z. B., and Guo, Y. C. (2024). High-strength and high-toughness alkali-activated composite materials: optimizing mechanical properties through synergistic utilization of steel slag, ground granulated blast furnace slag, and fly ash. *Constr. Build. Mater.* 422, 135811. doi:10.1016/j.conbuildmat.2024.135811

Malazdrewicz, S., Adam Ostrowski, K., and Sadowski, Ł. (2023). Self-compacting concrete with recycled Coarse aggregates from concrete construction and demolition waste – current state-of-the art and perspectives. *Constr. Build. Mater.* 370, 130702. doi:10.1016/j.conbuildmat.2023.130702

Mohammed, A. A., Ahmed, H. U., and Mosavi, A. (2021). Survey of mechanical properties of geopolymer concrete: a comprehensive review and data analysis. *Materials* 14, 4690. doi:10.3390/ma14164690

Nodehi, M., and Taghvaee, V. M. (2022a). "*Applying circular economy to construction industry through use of waste materials: a review of supplementary cementitious materials, plastics, and ceramics,*"(Berlin/Heidelberg, Germany: Springer International Publishing). 2, 987–1020. doi:10.1007/s43615-022-00149-x

Nodehi, M., and Taghvaee, V. M. (2022b). Alkali-activated materials and geopolymer: a review of common precursors and activators addressing circular economy. *Circ. Econ. Sustain.* 2, 165–196. doi:10.1007/s43615-021-00029-w

Ralegaonkar, R. V., Gavali, H. R., Sakhare, V. V., Puppala, A. J., and Aswath, P. B. (2017). Energy-efficient slum house using alternative materials. *Proc. Inst. Civ. Eng. Energy* 170, 93–102. doi:10.1680/jener.16.00027

Ram, S., Ralegaonkar, R. V., and Gavali, H. R. (2018). Assessment of energy efficiency in buildings using synergistic walling material. *Proc. Inst. Civ. Eng. Energy* 171, 182–189. doi:10.1680/jener.17.00029

Robayo-Salazar, R., Mejía-Arcila, J., Mejía de Gutiérrez, R., and Martínez, E. (2018). Life cycle assessment (lca) of an alkali-activated binary concrete based on natural volcanic pozzolan: a comparative analysis to OPC concrete. *Constr. Build. Mater.* 176, 103–111. doi:10.1016/j.conbuildmat.2018.05.017

Sathvik, S., Shakor, P., Hasan, S., Awuzie, B. O., Singh, A. K., Rauniyar, A., et al. (2023). Evaluating the potential of geopolymer concrete as a sustainable alternative for thin white-topping pavement. *Front. Mater.* 10, 1–14. doi:10.3389/fmats.2023.1181474

Scrivener, K. L., John, V. M., and Gartner, E. M. (2018). Eco-efficient cements: potential economically viable solutions for a low-CO2 cement-based materials industry. *Cem. Concr. Res.* 114, 2–26. doi:10.1016/j.cemconres.2018.03.015

Shelote, K. M., Gavali, H. R., Bras, A., and Ralegaonkar, R. V. (2021). Utilization of Co-fired blended ash and chopped basalt fiber in the development of sustainable mortar. *Sustain* 13, 1247. doi:10.3390/su13031247

Supriya, R., Chaudhury, R., Sharma, U., Thapliyal, P. C., and Singh, L. (2023). Low-CO2 emission strategies to achieve net zero target in cement sector. *J. Clean. Prod.* 417, 137466. doi:10.1016/j.jclepro.2023.137466

Tambara Júnior, L. U. D., Taborda-Barraza, M., Cheriaf, M., Gleize, P. J. P., and Rocha, J. C. (2022). Effect of bottom ash waste on the rheology and durability of alkali activation pastes. *Case Stud. Constr. Mater.* 16, e00790. doi:10.1016/j.cscm.2021.e00790

Tiwari, P. (2001). Energy efficiency and building construction in India. *Build. Environ.* 36, 1127–1135. doi:10.1016/S0360-1323(00)00056-1

United nation(2018). 68% of the world population projected to live in urban areas by 2050, says UN. Available online at: h t t p s : / / w w w . u n . o r g / development/desa/en/news/population/2018-revision-of-world-urbanization-prospects.html.

Unis Ahmed, H., Mahmood, L. J., Muhammad, M. A., Faraj, R. H., Qaidi, S. M. A., Hamah Sor, N., et al. (2022). Geopolymer concrete as a cleaner construction material: an overview on materials and structural performances. *Clean. Mater.* 5, 100111. doi:10.1016/j.clema.2022.100111

Wang, Y., Tang, C., Wang, M., Yu, Y., and Chen, S. (2024). Early mechanical properties and strength calculation method of slag-based alkali activated concrete. *AIP Adv.* 14. doi:10.1063/5.0194129

Wimbadi, R. W., and Djalante, R. (2020). From decarbonization to low carbon development and transition: a systematic literature review of the conceptualization of moving toward net-zero carbon dioxide emission (1995–2019). *J. Clean. Prod.* 256, 120307. doi:10.1016/j.jclepro.2020.120307

Yang, G., Zhao, J., and Wang, Y. (2022). Durability properties of sustainable alkali-activated cementitious materials as marine engineering material: a review. *Mater. Today sustain.* 17, 100099. doi:10.1016/j.mtsust.2021.100099

Yoo, D. Y., Banthia, N., You, I., and Lee, S. J. (2024). Recent advances in cementless ultra-high-performance concrete using alkali-activated materials and industrial byproducts: a review. *Cem. Concr. Compos.* 148, 105470. doi:10.1016/j.cemconcomp.2024.105470

Yurt, Ü., and Bekar, F. (2022). Comparative study of hazelnut-shell biomass ash and metakaolin to improve the performance of alkali-activated concrete: a sustainable greener alternative. *Constr. Build. Mater.* 320, 126230. doi:10.1016/j.conbuildmat.2021.126230